Original Article

Institution of MECHANICAL ENGINEERS
Journal of RAIL AND RAPID TRANSIT

Proc IMechE Part F:
J Rail and Rapid Transit
2018, Vol. 232(4) 1078–1087

DOI: 10.1177/0954409717707834
journals.sagepub.com/home/pif
SAGE

Influence of toe load on the fatigue resistance of elastic rail clips

Anat Hasap[1], Phanasindh Paitekul[1], Nitikorn Noraphaiphipaksa[2] and Chaosuan Kanchanomai[2]

Abstract

As a critical component of the fastening system, the elastic rail clip maintains the rail in the vertical, lateral, and longitudinal positions using its specified toe load. In this study, the influence of toe load on the deformation and fatigue resistance of the clip was studied. Finite element analysis, static load experiments, and fatigue experiments were performed to evaluate the deformation and fatigue resistance of the clip. With the contribution of the lateral wheel load, the deformation range of the outer clip was higher than that of the inner clip. Therefore, the cyclic deformation of the outer clip was used for the fatigue experiment. The toe load had no influence on the fatigue resistance of the clip under normal wheel load, i.e. the clips under high, normal, and low toe loads were run-out at 5×10^6 cycles. However, with the contribution of impact on the wheel load, the fatigue lives were reduced to 5468 cycles and 16,839 cycles for the clips under high and normal toe loads, respectively. In the case of low toe load, the clip under the contribution of impact could withstand more than 5×10^6 cycles. Accordingly, the reduction of toe load may enhance the fatigue resistance of the clip under impact.

Keywords

Elastic rail clip, toe load, wheel load, fatigue, fastening system

Date received: 23 November 2016; accepted: 2 April 2017

Introduction

In the modern railway track system, various components – e.g. rail, pad, insulator, clip, and base plate – form a complex fastening system.[1,2] One critical component of the fastening system is the clip, which properly maintains the rail in vertical, lateral, and longitudinal positions. An important criterion to ensure the proper functioning of the clip is the specified toe load during the installation. In order to ensure a proper toe load, the load transducer has been invented and successfully employed in the load measurement. It was found that some clips have toe loads that differ from the specification. Moreover, clips in service are subjected to the combination between the toe load (static load) and the repeated wheel load (cyclic load), which can cause fatigue failure.[3] Because the high static load can accelerate the fatigue failure of engineering components,[3] it is therefore necessary to systematically investigate the influence of the toe load on the fatigue failure of the clip.

Mohammadzadeh et al.[4] proposed a method for the analysis of fatigue reliability of the fastening spring clip under operating conditions. The displacement–time history was applied to the finite element analysis (FEA) of the fastening spring clip. The crack nucleation life was numerically estimated using the rain-flow method and Palmgren–Miner linear damage rule. Unfortunately, the in-service fatigue lives were not compared with their results to verify the predictions. Tamagawa et al.[5] developed a fatigue limit diagram for the "wire-shaped" clip, i.e. the relationship between the mean strain and the strain amplitude. Their fatigue life predictions using a fatigue limit diagram were in good agreement with those of fatigue tests. Sadeghi et al.[6] experimentally evaluated the influence of the rail loading conditions on the fatigue phenomena of Vossloh and Pandrol flexible clips under various train speeds and axle loads. The increase of axle loads caused substantial increases in the plastic deformations of the clips, while the train speeds had less influence on the deflection.

[1]Railway Transportation System Testing Center, Institute of Scientific and Technological Research, Pathumthani, Thailand
[2]Faculty of Engineering, Department of Mechanical Engineering, Center of Materials Engineering and Performance, Thammasat University, Pathumthani, Thailand

Corresponding author:
Chaosuan Kanchanomai, Department of Mechanical Engineering, Faculty of Engineering, Thammasat University, Pathumthani 12120, Thailand.
Email: kchao@engr.tu.ac.th

A comparison of the results obtained for the two types of clips (Vossloh and Pandrol) indicated that both the railway flexible clips had the similar fatigue behavior. Shang et al.[7] numerically evaluated the effect of the vertical displacement of the clip's finger on the clamping force and stress. The vertical displacement of the clip's finger had a marginal effect on the clamping force, but a large effect on the maximum equivalent stress in the clip. The fatigue crack might easily nucleate and propagate in the clip's stress concentration area after repeated passages of trains. Although there are literature works that focus on the reliability of clips, the effect of toe load on the reliability of the clip has not been clearly understood.

In this study, the influence of toe load on the deformation and fatigue resistance of elastic rail clips was studied. FEA, static load experiments, and fatigue experiments were performed to evaluate the deformations and fatigue resistances of clips. The findings can be used as a guideline for the installation and maintenance to ensure the structural integrity of a railway track system.

Railway track system

An elastic rail clip (e-clip), which is a standard type of elastic rail fastening, was used in this study. The clip applies the toe load between the rail and the sleeper to prohibit the relative movement (Figure 1). Its chemical composition was evaluated using an emission spectrometer (Spectrolab: M10), i.e. 0.532 wt% C, 1.80 wt% Si, 0.841 wt% Mn, 0.244 wt% Cr, and 96.1 wt% Fe. The composition corresponds to that of the SUP10 spring steel (JIS G4801[8]). On the other hand, the rail was an UIC60 rail (BS EN 13674[9]).

Procedure of the research

FEA, static load experiments, and fatigue experiments were performed to evaluate the deformations and

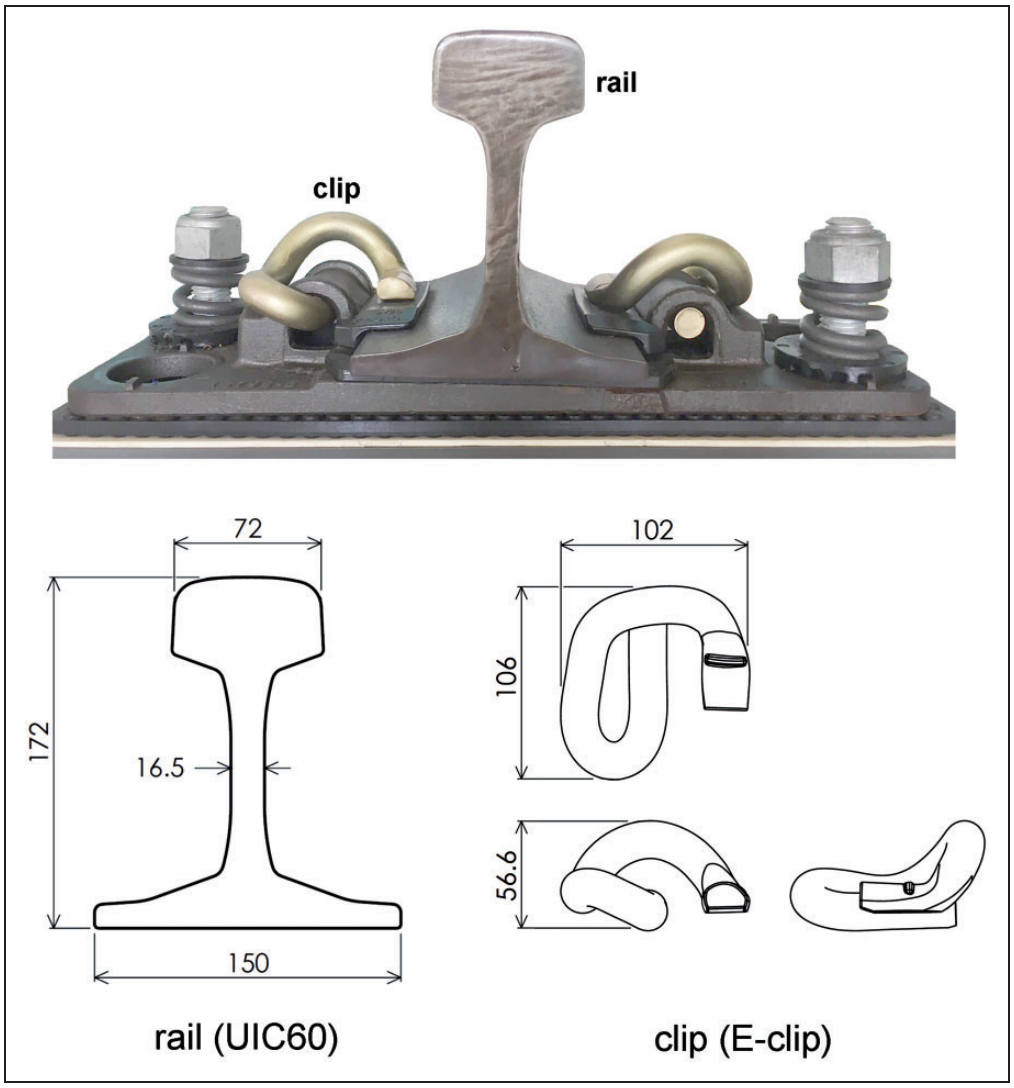

Figure 1. The railway track system (dimension in mm).

fatigue resistances of clips. The study was divided into four steps as follows:

(i) *Deformation of the railway track system*. The stresses and deformations of a railway track system with five base plates under the combination of toe load and wheel load were experimentally and numerically evaluated. FEA results were then compared with those of experiments to validate the FEA.
(ii) *Influence of the number of base plates on the deformation of rails*. The deformations of rails with various lengths and number of base plates under wheel load were numerically calculated. The length and number of base plates, that properly represent the deformation of rail, were selected for the evaluation of clip deformation.
(iii) *Deformation of clips*. The deformations of the railway track system under the combination of toe load and wheel load were numerically calculated using FEA. The maximum deformation range of clip was determined and used as a cyclic deformation for the fatigue experiment of the clip.
(iv) *Fatigue of clips*. The fatigue experiments of clips were performed to evaluate the fatigue resistance of clips.

Deformation of the railway track system

Static loading experiment

The experimental set-up for the deformation of the railway track system with five base plates is shown in Figure 2. The bolt load of 2.5 kN was applied on each side of the base plate to keep the base plate on the rigid surface (Figure 3(a)). In a fastening system, a clip was clamped between the insulator and the base plate with the rail and rail pad in the middle, i.e. the toe load was induced on the clip. Based on the stiffness of the clip (1.1 kN/mm), the outer toe load was 1.07 kN, while the inner toe load was 1.03 kN. Subsequently, two wheel loads, i.e. 74-kN compressive loads, were simultaneously applied to the top of the rail using a servo hydraulic actuator (Samyeon: STC-50D with 500-kN load cell).

Two cases of wheel loads (wheel loads A and B, Figure 3(a)) were applied in this work. Wheel load A represented the situation when one of the wheels was on the base plate, while wheel load B represented the situation when one of the wheels was at the middle between two base plates. The distance between the wheel loads (wheel span) was 1500 mm, while the distance between the base plates was 600 mm. The loading rate was 20 kN/min. The temperature and relative humidity during the static loading experiment were controlled at $30 \pm 2^{\circ}$C and $60 \pm 5\%$, respectively. It is noted that these loads and spans were used only for the laboratory setup and FEA validation.

The strain on the rail along the longitudinal direction and at the middle between the base plates was measured using a quarter-bridge strain gauge (TML: FLA-03-11). The strain gauge measurement had a precision of 0.5 μm/m. The deformation of the rail

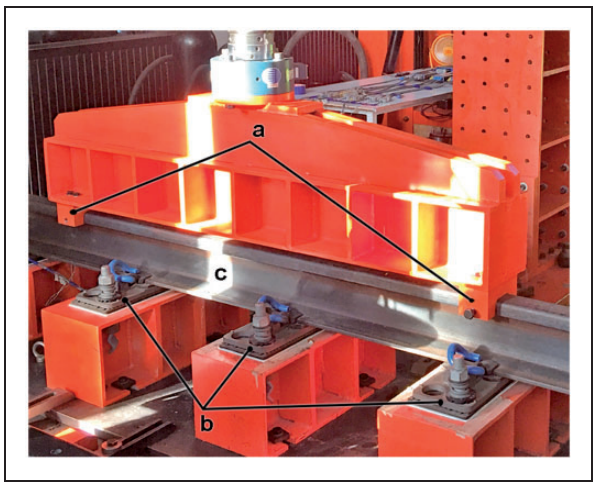

Figure 2. The experimental set-up for the deformation of railway track system with five base plates (a – wheel loads, b – base plates, and c – rail).

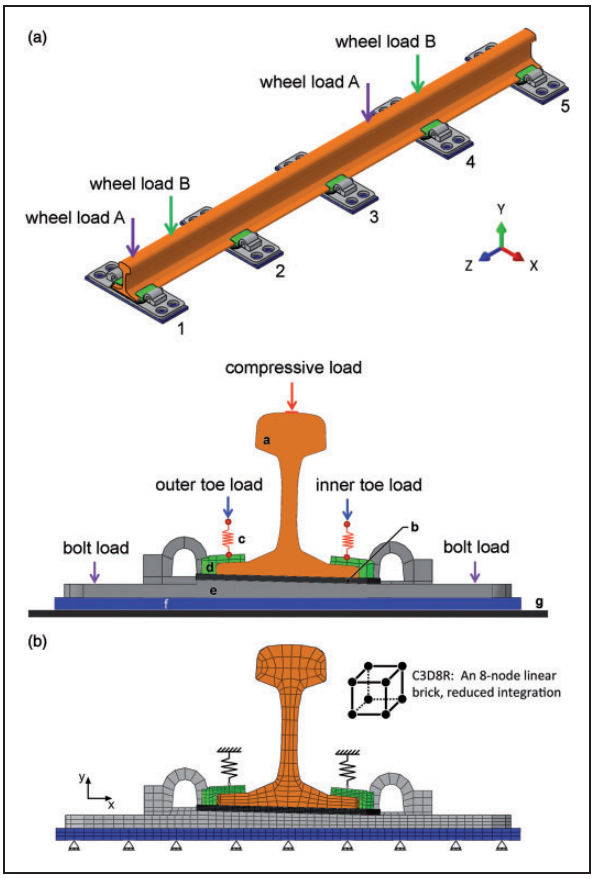

Figure 3. The railway track system with five base plates: (a) schematic illustrations (a: rail; b: rail pad; c: clip; d: insulator; e: base plate; f: rubber pad; and g: rigid surface) and (b) FEA model.

in the vertical direction and at the middle between the base plates was measured using a dial gauge with a precision of 10 μm. It is noted that the deformation measured by the dial gauge was a combination of the deformations of the rail and the rail pad. The strain was converted to stress using Hook's law. Both stresses and deformations obtained from the experiments were used to validate the FEA.

Table 1. Components of the railway track system.

Component	Type	Material	Elastic modulus (GPa)
Rail	UIC60	Steel	210
Rail pad	UIC60	EVA	20
Clip	e-clip	SUP10	210
Insulator	UIC60	Nylon: PA66	23
Base plate	UIC60	Cast iron	210
Rubber pad	UIC60	Rubber	10

Table 2. Elements of the railway track system with five base plates.

Component	Element type	Element size (mm)	Number of elements
Rail	C3D8R	1.4–14	25,920
Rail pad	C3D8R	0.6–6	17,120
Clip	spring	–	10
Insulator	C3D8R	0.5–5	4520
Base plate	C3D8R	0.8–8	22,320
Rubber pad	C3D8R	0.8–9	23,300

Finite element analysis

The stresses and deformations of a railway track system with five base plates under the combination of toe load and wheel load were numerically calculated using 3D linear-elastic FEA, i.e. ABAQUS.[10] Bolt loads applied for FEA were similar to those of the static loading experiment. To simplify the FEA model, the clips were replaced by linear springs with the same stiffness of 1.1 kN/mm, as shown in Figure 3(b). The material properties of each component are shown in Table 1. It is assumed that the Poisson's ratios (ν) of steel components were 0.3, while those of polymer components were 0.45. The deformation and compressive load of linear springs were adjusted to be the same as those of clips after installation, i.e. the outer toe load of 1.07 kN, and the inner toe load of 1.03 kN. Two cases of wheel loads (wheel loads A and B) were applied for FEA.

Frictional-contact elements (eight-node linear brick, C3D8R), master-slave algorithm, and penalty method were applied to all the contact interfaces. They are the contacts between rail vs. rail pad, rail vs. insulator, rail pad vs. base plate, base plate vs. rubber pad, and rubber pad vs. rigid surface.

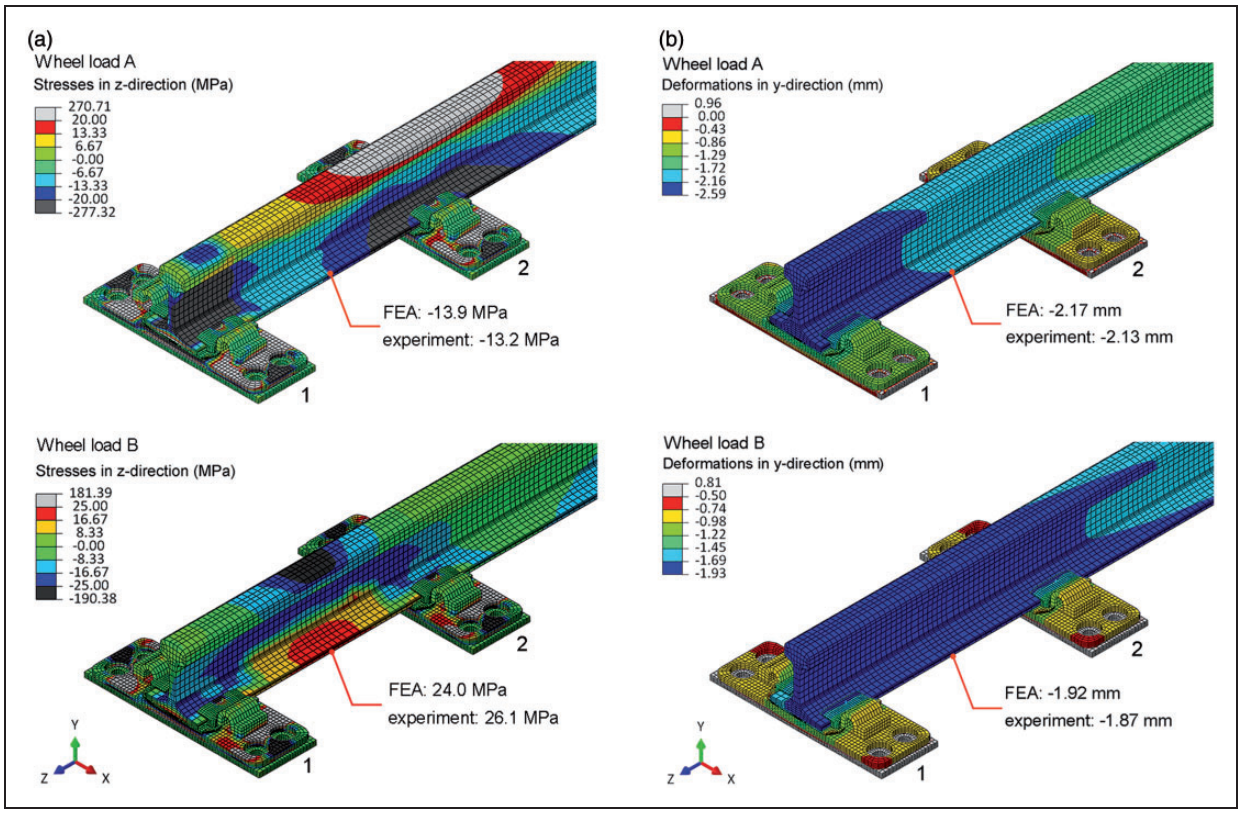

Figure 4. The railway track system with five base plates: (a) stresses and (b) deformations.

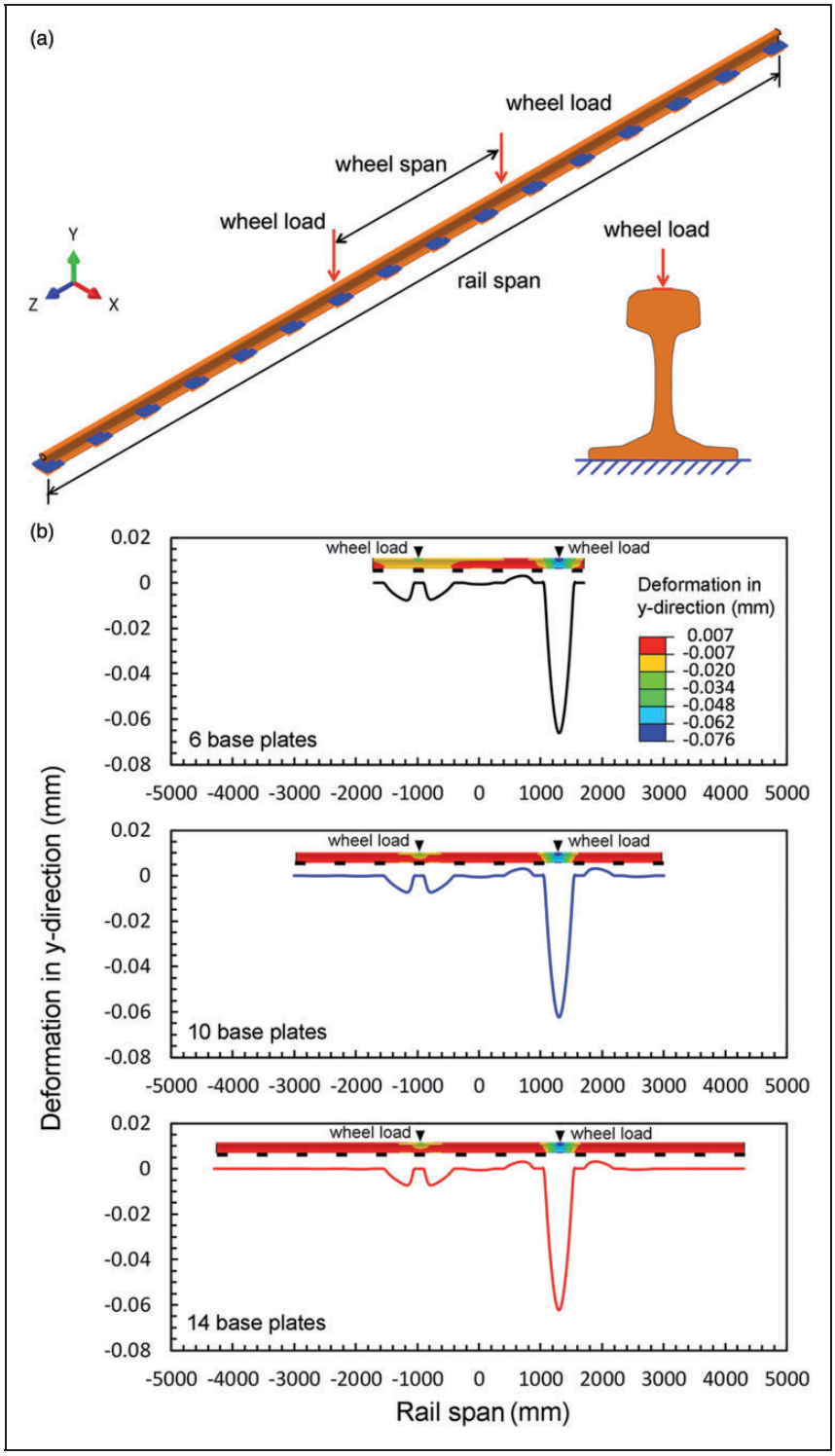

Figure 5. Rail and rigid supports at the locations of base plates: (a) schematic illustrations and (b) deformations in the vertical direction (*y*-axis) of the rail.

The slip of the contact interface was assumed to occur when the shear stress is greater than the critical shear stress (τ_c), i.e.

$$\tau \geqslant \tau_c = \mu\sigma_n \tag{1}$$

where σ_n and μ are the normal stress and the friction coefficient, respectively. The friction coefficient of 0.3 was assumed for all contacts. The boundary conditions were applied at the contact between the rubber pad and the rigid surface. The displacement in the y direction and the rotations around all axes were constrained. Each wheel load was gradually increased with intervals of 20 steps from 0 to the maximum of 74 kN. To minimize the influence of element size, the size of elements was adjusted until the variation of the

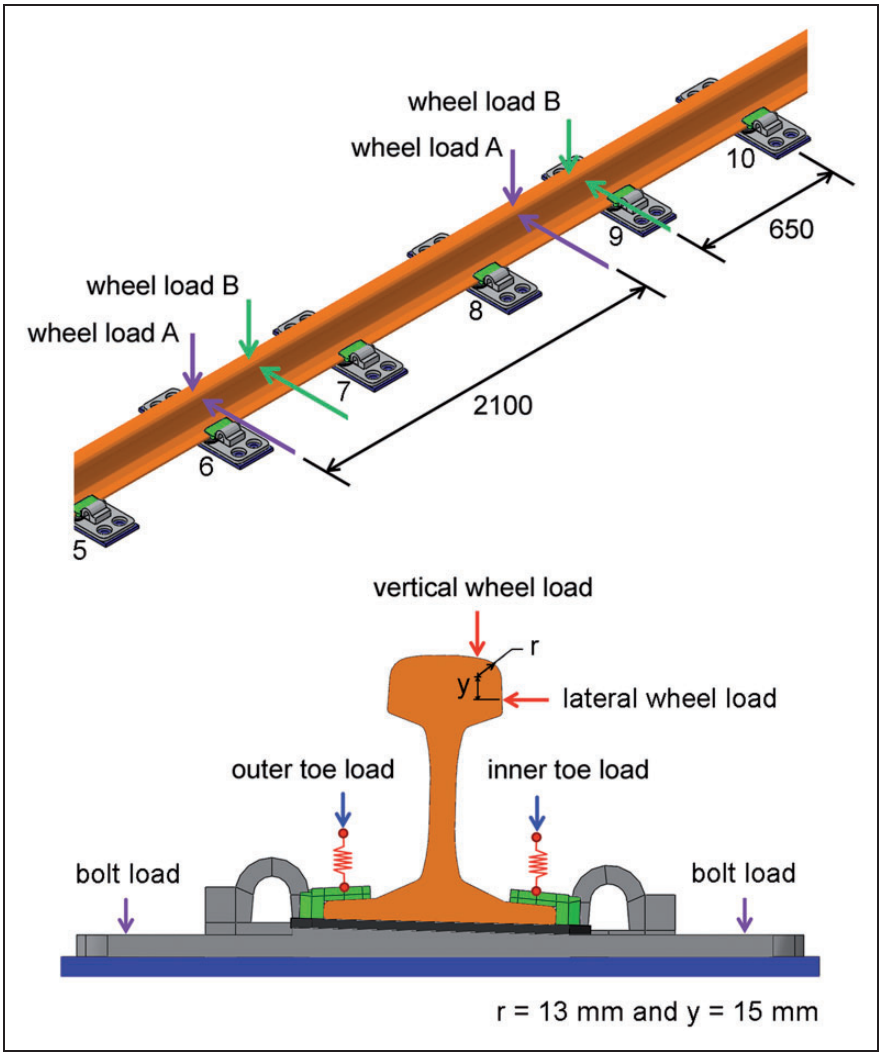

Figure 6. Schematic illustrations of the railway track system with 15 base plates (showing base plate nos 5–10, and dimension in mm).

Von Mises stress around the critical points of each component was below 5%. The sizes of the element and the number of elements of each component are summarized in Table 2.

The stresses and deformations of a railway track system with five base plates obtained from experiments and FEA are shown in Figure 4(a) and (b), respectively. The stresses and deformations calculated using FEA were in good agreement with those of experiments. Thus, the validation of the present FEA was confirmed.

Influence of the number of base plates on the deformation of rails

Because the length of the rail and the number of base plates could influence the deformations of rail and clips under wheel load, the deformations of rails with various lengths and number of base plates (up to 14 base plates) were numerically calculated. The length of the rail and the number of base plates that clearly represent the deformation of rail should be used for the numerical evaluation of deformations of clips.

It is known that the flexibility of the fastening system has influence on the stress and deformation of rail. Thus, the deformations of rails with various lengths and number of base plates should be evaluated using the model with fastening system. Unfortunately, models with various lengths and number of base plates have too many assemblies of complex parts and require long run time. To simplify the FEA model, only rail and rigid supports at the locations of base plates were used for the FEA (Figure 5(a)). Although this simplification cannot provide the actual stress and deformation of rails, it is believed that the results of FEA can be used for the selection of the length of the rail and the number of base plates to be used for the numerical evaluation of deformations of clips.

The number of base plates used for the FEA were 6, 10, and 14. The actual wheel span (2100 mm) and base plate span (650 mm) were used for the FEA. The material property, element, and boundary conditions

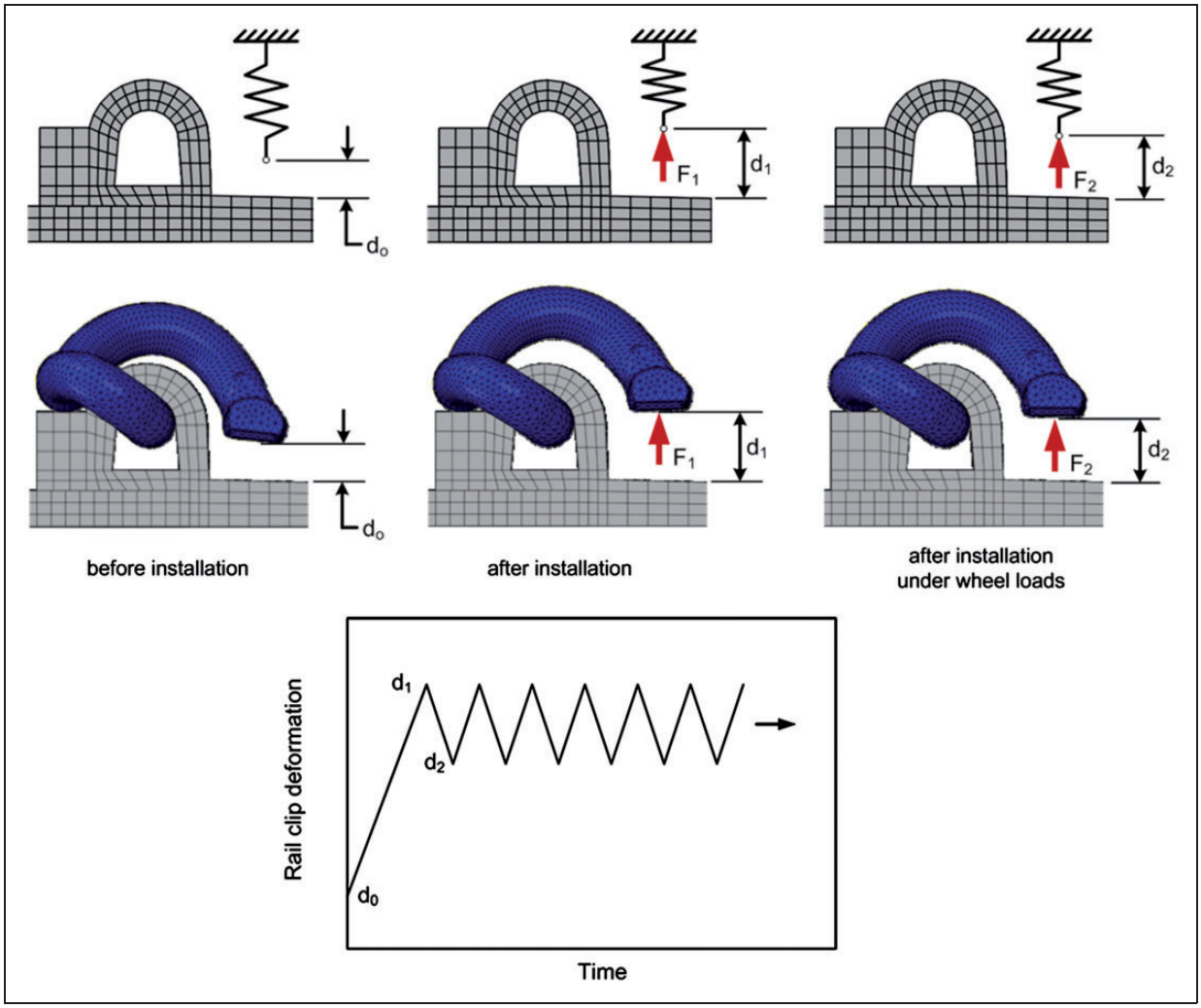

Figure 7. Schematic illustrations of the deformation of the clip.

were similar to the previous FEA (section "Finite element analysis"). Wheel load A, which represented the situation when one of the wheels was on the base plate, was used for the FEA.

Deformations in the vertical direction of the rail (*y*-axis) are shown in Figure 5(b). Because the left wheel load was applied on the base plate, the deformation of rail was limited. On the other hand, the right wheel load was applied between base plates; thus, the highest deformation of the rail could be observed. FEA model with 14 base plates clearly represented the deformations of rail under two wheel loads; thus an FEA model with 14 base plates or more should be used for the numerical evaluation of clip deformations.

Deformation of clips

Stresses and strains of the railway track system under the combination of toe load and wheel load were numerically calculated. The maximum deformation range of the clip was determined and used as cyclic deformation for the fatigue experiment of the clip. A railway track system with 15 base plates was selected for the FEA, as shown in Figure 6. Geometries, material properties, elements, bolt load, outer toe load, inner toe load, and boundary conditions were similar to the previous FEA (section "Finite element analysis"). However, the distance between wheels was 2100 mm, while the distance between base plates was 650 mm. These wheel span and base plate span were selected to represent the actual geometries of the railway track system. To simulate the curve rail, where most of the clip failure was observed,[1] a lateral wheel load of 39 kN and a vertical wheel load of 74 kN were used for the FEA. These loads were suggested by AS 1085.19[11] for the curve rail in the mainline of a 20-ton axle load vehicle at a speed of 100 km/h, which is similar to those recommended by BS EN 13481.[12]

Schematic illustrations of the clip deformation are shown in Figure 7, where d_o is the distance from the upper surface of the base plate to the clip before installation, F_1 and d_1 are the toe load and distance from the upper surface of base plate to the clip after installation, and F_2 and d_2 are the toe load and distance between the upper surface of base plate to the clip under wheel loads. Because a clip is under the

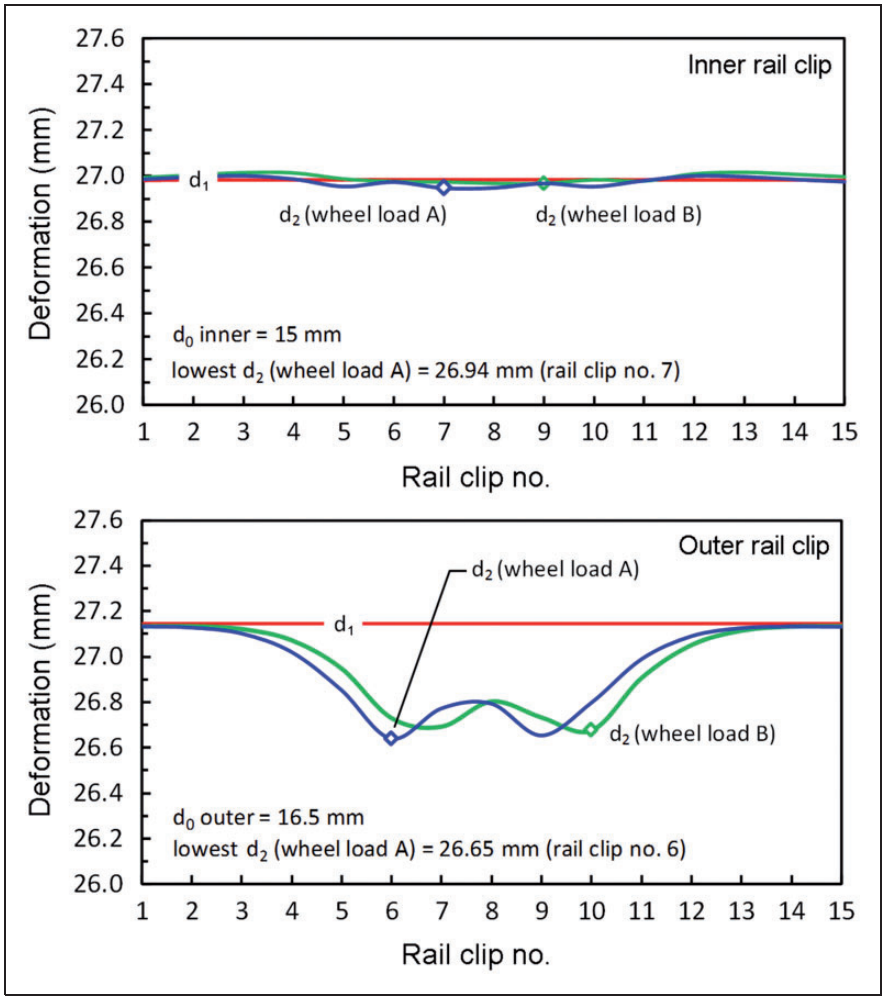

Figure 8. Deformations of clips under wheel loads A and B.

repeated wheel loads during actual operation, the cyclic deformation from d_1 to d_2 is likely to occur, as schematically shown in Figure 7. If the magnitude of deformation and number of cycles are high enough, the fatigue failure of clip is possible.

Deformations of the inner and outer clips under wheel loads A and B are shown in Figure 8. With the contribution of the lateral wheel load, the d_2 of outer clips were lower than those of inner clips, i.e. the deformation ranges of outer clips were higher than those of inner clips. Under wheel load A, the left wheel load was applied on the rail above base plate no. 6 (Figure 6); therefore, the lowest d_2 at outer clip no. 6 was lower than that under wheel load B. Because the cyclic deformation of outer clip no. 6 was most severe, i.e. $d_o = 16.50$ mm, $d_1 = 27.15$ mm, and $d_2 = 26.65$ mm, the fatigue resistance of this clip should be the lowest. Thus, the cyclic deformation of outer clip no. 6 was used as the cyclic deformation for the fatigue experiment of clips.

Fatigue of clips

A combination of toe load (static load) and repeated wheel load (cyclic load) can cause fatigue failure[3]; thus, the cyclic deformation of clips due to the toe load and wheel load was simulated during fatigue experiment. To obtain a broad analysis, the toe loads under three installation conditions were evaluated, i.e. low, normal, and high toe loads. The cyclic deformation for the fatigue experiment under normal toe load (i.e. normal clip installation) was obtained from the FEA of the previous section. However, the clip may be under-deformed or over-deformed during installations. To simulate the low

Table 3. Deformations and fatigue lives of clips.

Clip deformation				
Wheel load	Toe load	d_1 (mm)	d_2 (mm)	Fatigue life (cycle)
Normal	Normal	27.15	26.65	$>5 \times 10^6$
	High	29.15	28.65	$>5 \times 10^6$
	Low	25.15	24.65	$>5 \times 10^6$
Impact	Normal	27.15	26.35	16,839
	High	29.15	28.35	5468
	Low	25.15	24.35	$>5 \times 10^6$

$d_0 = 16.50$ mm for all cases of fatigue experiment.

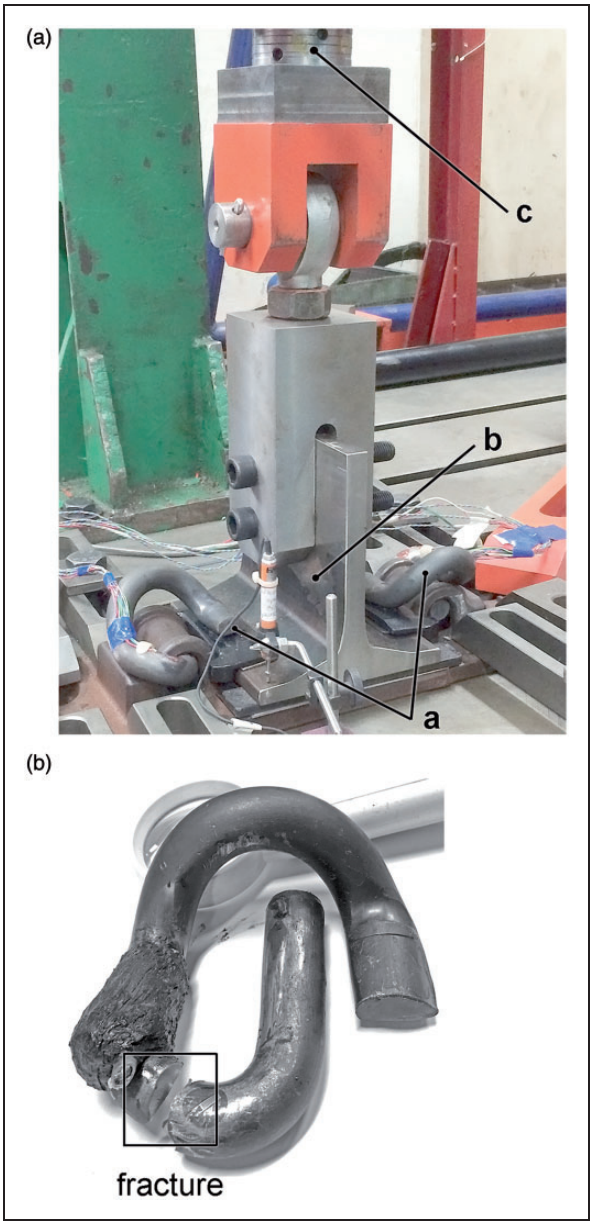

Figure 9. (a) The experimental set-up for the fatigue of clip (a: clips; b: rail; and c: actuator) and (b) location of fracture.

toe load (i.e. under-deformed clip installation) the deformation of 2 mm was subtracted from the deformations of the clip under normal installation (d_1 and d_2), while the deformation of 2 mm was added to the deformations of the clip under normal installation (d_1 and d_2) to simulate the high toe load (i.e. over-deformed clip installation). The deformations of clips under the influence of toe loads are summarized in Table 3.

In the actual operation of a railway track system, the impact caused by irregularities of rails and wheels, e.g. weldment, wear, corrugated rail, can add up to 60% of the wheel load.[4,13] Ling et al.[13] found that the Von Mises stress increased with the corrugation depth. For severe corrugation, the Von Mises stress in the clip exceeded the ultimate strength of the clip due to the impact load. To simulate the influence of impact on cyclic deformation, 60% of deformation was added to the cyclic deformation range (d_1–d_2), while the deformation under toe load (d_1) was unaltered. The deformations of clips under the influence of impact are summarized in Table 3.

The experimental set-up for the fatigue of the clip is shown in Figure 9(a). Two clips were clamped between the insulators and the base plate with the rail and rail pad in the middle. Sinusoidal cyclic deformation with 5 Hz frequency was applied to the clips through a rail by a servo hydraulic actuator (MTS: 244.22 with 100 kN load cell). A linear-variable differential transformer with 0.05-mm precision was used to control the required deformation of the clip. The temperature and relative humidity during the fatigue experiment were controlled at $30 \pm 2^{\circ}C$ and $60 \pm 5\%$, respectively. The fatigue life is defined as the number of cycles that occur before a complete fracture. However, if a clip does not fail after 5×10^6 cycles, it is considered as a run-out. With three cases of toe loads and two cases of wheel loads (Table 3), the fatigue experiments were performed under six conditions. The fatigue experiments were repeated twice for each condition, and the average fatigue lives were determined. The difference in fatigue lives between repeated fatigue experiments was lower than 10%. However, this difference and uncertain factors during fatigue experiments may be minimized by increasing the number of repeated experiments.

The experimental results are summarized in Table 3. Under normal wheel load, the toe load had no influence on the fatigue resistance of the clip, i.e. the clips under high, normal, and low toe loads were run-out. However, with the contribution of an impact, the fatigue lives were significantly reduced to 5468 cycles and 16,839 cycles for the clips under high and normal toe loads, respectively. In both cases, the fractures of clips occurred at the same location, i.e. fatigue crack started from the inner curvature and propagated to the outer curvature (Figure 9(b)). Under low toe load with impact, the clip could withstand more than 5×10^6 cycles. Based on these findings, it is recommended that the proper maintenance of a railway track system is crucial to keep the impact as low as possible. If all maintenances are appropriately carried out but the fatigue is still prevalent, a possible solution is to reduce the toe load, as it showed the positive effect on the fatigue resistance of the clip under impact. However, the reducing of toe load has disadvantages, and should be carefully considered. If the toe load of the clip is reduced too much, the clip may not be able to properly maintain the rail in vertical, lateral, and longitudinal positions, i.e. the fastening system becomes loose. Under this situation, the slips and vibrations may develop among the components of the fastening system, which may enhance the deterioration of each component.

Conclusion

FEA, static load experiments, and fatigue experiments were performed to evaluate the influence of toe load on the deformation and fatigue resistance of clips. The findings are summarized as follows:

1. Stresses and deformations calculated using FEA were in good agreement with those of experiments. The FEA model with 14 base plates or more clearly represented the deformations of rail under wheel loads; thus, the FEA models with 15 base plates were used for the numerical evaluation of clip deformations.
2. With the contribution of the lateral wheel load, the deformation ranges of outer clips were higher than those of inner clips. Therefore, the cyclic deformation of the outer clip was used as cyclic deformation for the fatigue experiment.
3. The toe load had no influence on the fatigue resistance of the clip under normal wheel load, i.e. the clips under high, normal, and low toe load were run-out after 5×10^6 cycles. However, with the contribution of impact, the fatigue lives were significantly reduced to 5468 cycles and 16,839 cycles for the clips under high and normal toe loads, respectively. Under low toe load with impact, the clip could withstand more than 5×10^6 cycles.

Acknowledgements

The authors would like to acknowledge the discussion and support from Dr Anchalee Manonukul (National Metal and Materials Technology Center, Thailand).

Declaration of Conflicting Interests

The author(s) declared no potential conflicts of interest with respect to the research, authorship, and/or publication of this article.

Funding

The author(s) disclosed receipt of the following financial support for the research, authorship, and/or publication of this article: The authors would like to acknowledge the supports from the Thammasat Research Fund, the Thailand Commission on Higher Education of Thailand (the National Research University Project), the Royal Golden Jubilee Ph.D. Program (RGJ), the Thailand Research Fund (TRF), and the National Research Council of Thailand (NRCT).

References

1. Esveld C. *Modern railway track*. Zaltbommel, The Netherlands: MRT-Productions, 2001, p.189.
2. Esveld C. Recent developments in slab track. *Eur Railway Rev* 2003; 2: 81–85.
3. Suresh S. *Fatigue of materials*. 2nd edn. Cambridge: Cambridge University Press, 1998.
4. Mohammadzadeh S, Ahadi S and Nouri M. Stress-based fatigue reliability analysis of the rail fastening spring clip under traffic loads. *Latin Am J Solids Struct* 2014; 11: 993–1011.
5. Tamagawa S, Kataoka H and Deshimaru T. A fatigue limit diagram for plastic rail clips. *WIT Trans Built Environ* 2014; 135: 839–848.
6. Sadeghi J, Fesharaki M and Khajehdezfuly A. Influences of train speed and axle loads on life cycle of rail fastening clips. *Trans Can Soc Mech Eng* 2015; 39: 1–11.
7. Shang HX, Wen ZF, Wu L, et al. Finite element analysis of type III rail fastening clip failure in metro lines. *Gongcheng Lixue/Eng Mech* 2015; 32: 210–215.
8. JIS G 4801. *Spring steels*. Tokyo, Japan: The Japan Iron and Steel Federation, 2011.
9. BS EN 13674-1. Railway applications – track – Vignole railway rails 46 kg/m and above. In: *British-Adopted European Standard*. Brussels, Belgium: European Committee for Standardization, 2002.
10. *ABAQUS user's manual*. Providence, Rhode Island, USA: Dassault Systémes Simulia Corp., 2014.
11. AS1085.19. Railway track material. In: *The Australian standard*. Sydney, Australia: Standards Australia International Ltd, 2003.
12. BS EN 13481-2. Railway applications – track – performance requirements for fastening systems. Fastening systems for concrete sleepers. In: *British-Adopted European Standard*. Brussels, Belgium: European Committee for Standardization, 2012.
13. Ling L, Li W, Shang H, et al. Experimental and numerical investigation of the effect of rail corrugation on the behaviour of rail fastenings. *Vehicle Syst Dyn* 2014; 52: 1211–1231.